

---

# InfoTok: Regulating Information Flow for Capacity-Constrained Shared Visual Tokenization in Unified MLLMs

---

Lv Tang<sup>1</sup> Tianyi Zheng<sup>2</sup> Bo Li<sup>2</sup> Xingyu Li<sup>1</sup>

## Abstract

Unified multimodal large language models (MLLMs) integrate image understanding and generation in a single framework, with the visual tokenizer acting as the sole interface that maps visual inputs into tokens for downstream tasks. However, existing shared-token designs are mostly architecture-driven and lack an explicit criterion for what information tokens should preserve to support both understanding and generation. Therefore, we introduce a capacity-constrained perspective, highlighting that in shared-token unified MLLMs the visual tokenizer behaves as a compute-bounded learner, so the token budget should prioritize reusable structure over hard-to-exploit high-entropy variations and redundancy. Motivated by this perspective, we propose **InfoTok**, an information-regularized visual tokenization mechanism grounded in the Information Bottleneck (IB) principle. InfoTok formulates tokenization as controlling information flow from images to shared tokens to multimodal outputs, yielding a principled trade-off between compression and task relevance via mutual-information regularization. We integrate InfoTok into three representative unified MLLMs without introducing any additional training data. Experiments show consistent improvements on both understanding and generation, supporting information-regularized tokenization as a principled foundation for learning a shared token space in unified MLLMs.

## 1. Introduction

Unified multimodal large language models (MLLMs) have advanced rapidly, aiming to support both image understanding and generation within a single framework (Wu et al.,

<sup>1</sup>University of Alberta, Department of Electrical and Computer Engineering, Edmonton, Canada <sup>2</sup>vivo Mobile Communication Co., Ltd, Shanghai, China. Correspondence to: Lv Tang <luckybird1994@gmail.com>.

2025a; Deng et al., 2025; Wu et al., 2025d;c; Huang et al., 2025; Ma et al., 2025; Han et al., 2025; Wu et al., 2025b; Lin et al., 2025a). A central bottleneck in this unification is the **visual tokenizer**, which converts high-dimensional images into a token sequence consumed by the LLM. However, understanding and generation impose conflicting requirements on the representation. Understanding favors compact semantic abstractions, while generation depends on retaining sufficient perceptual cues. This discrepancy has led to two dominant strategies, decoupled and shared tokenization, whose evolution reflects the field’s ongoing pursuit of representational balance in unified modeling.

Models like Janus (Wu et al., 2025a) and BAGEL (Deng et al., 2025) adopt decoupled visual encoders, using separate branches for understanding and generation. This separation mitigates cross-task interference by allowing each branch to specialize at an appropriate level of representational granularity. However, it departs from the goal of a truly shared representation and increases architectural complexity. Shared-token models construct a single token space for both tasks (Wu et al., 2025d;c; Huang et al., 2025; Ma et al., 2025; Han et al., 2025), for example by enlarging codebooks (Ma et al., 2025) or aligning visual tokens with text embeddings (Wu et al., 2025d). Despite their progress, existing shared-token methods remain largely architecture-driven. They rely on end-to-end task losses without an explicit criterion that specifies what information a shared visual token should preserve, leaving the notion of sufficiency for both understanding and generation unformalized.

Importantly, in shared-token unified MLLMs, the visual tokenizer operates under finite capacity and limited compute when compressing rich visual inputs into a shared token space, and thus behaves as a compute-bounded learner. Under this constraint, not all visual information is equally useful. Many low-level details behave like hard-to-exploit high-entropy variations that waste representational budget, whereas transferable capability is more closely tied to reusable structure such as semantic entities and compositional cues. We term this observation the capacity-constrained perspective. It motivates an explicit mechanism to regulate what shared tokens encode, shifting visual tokenization from indiscriminate compression to allocating representational budget toward reusable and structurally

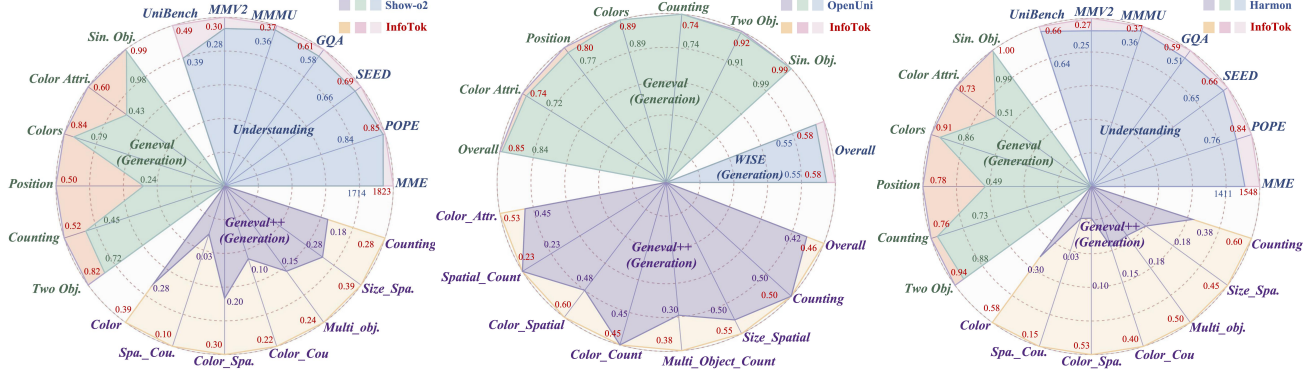


Figure 1. Performance comparison of three representative unified MLLMs (Show-o2 (Xie et al., 2025b), OpenUni (Wu et al., 2025b) and Harmon (Wu et al., 2025c)) before and after applying InfoTok regularization. Each radar chart reports results across representative image understanding benchmarks (UniBench (Li et al., 2025), GQA (Hudson & Manning, 2019), SEED (Li et al., 2023a), POPE (Li et al., 2023c), MME (Fu et al., 2023), MMV2 (Yu et al., 2024) and MMMU (Yue et al., 2024)) and image generation benchmarks (Geneval (Ghosh et al., 2023), Geneval++ (Ye et al., 2025) and WISE (Niu et al., 2025)). The InfoTok-regularized variants achieve consistently improved balance between semantic understanding and visual synthesis, demonstrating that information-theoretic regularization effectively enhances representation sufficiency and cross-modal generalization in unified multimodal learning. All InfoTok fine-tuning experiments are conducted without introducing any additional datasets, relying solely on the original training data used by each baseline.

valuable information that the compute-bounded visual tokenizer in shared-token unified MLLMs can reliably exploit.

To translate above goal into a concrete objective, we propose **InfoTok**, an information-regularized visual tokenization framework for unified multimodal understanding and generation tasks. InfoTok treats shared tokenization as an explicit allocation problem under a limited representational budget, controlling the information flow from images to tokens to multimodal outputs so that the resulting tokens remain sufficient for both semantic abstraction and perceptual fidelity. Realizing this goal requires a computable criterion to regulate the trade-off, because otherwise the shared token space is determined implicitly by optimization dynamics and the balance between abstraction and fidelity becomes difficult to control. This motivates an information-theoretic formulation of shared tokenization. We adopt the Information Bottleneck (IB) principle (Tishby et al., 2000; Tishby & Zaslavsky, 2015) to express tokenization as a principled trade-off between compression and task relevance via mutual-information (MI) terms. However, computing these mutual information terms in closed form is generally infeasible, since the visual input and discrete tokens lie in heterogeneous spaces and the underlying distributions are inaccessible. To obtain a computable objective, we instantiate InfoTok with computable dependence estimators and adopt a variational IB (VIB) formulation (Alemi et al., 2017) to regulate the information dependencies during training. As a result, our proposed InfoTok promotes compact tokens that preserve reusable semantic and compositional structure, together with task-relevant perceptual cues.

We integrate InfoTok into three representative unified MLLMs, including Harmon (Wu et al., 2025c), OpenUni (Wu et al., 2025b), and Show-o2 (Xie et al., 2025b),

and fine tune them without additional training data. As shown in Fig. 1, InfoTok consistently enhances both understanding and generation performance, supporting our thesis that explicitly regulating information flow yields a more optimal and stable shared token space. Beyond empirical gains, we provide a theoretical analysis that further supports information regularized tokenization as a coherent foundation for shared token learning, and offers insight into the feasibility of unifying multimodal understanding and generation within a single representation.

Our contributions are summarized as follows:

- We introduce a capacity-constrained perspective for shared tokenization, highlighting that in shared-token unified MLLMs the visual tokenizer operates as a compute-bounded learner under limited representational capacity and computation, and thus requires an explicit criterion to allocate budget toward reusable structure rather than high-entropy visual variations.
- We ground shared token learning in an information-theoretic objective. Building on IB principle, we formalize InfoTok by modeling the information dependencies among visual inputs, shared tokens, and multimodal outputs, which yields an explicit regularization objective for shared visual tokenization.
- We integrate InfoTok into three representative unified MLLMs without additional training data and observe consistent gains on both understanding and generation, validating the effectiveness of information-regularized tokenization for unified multimodal learning. These results also suggest a practical path for translating the theory into the design of unified MLLM frameworks.

## 2. Related Work

Recent advances in MLLMs have spurred growing interest in unified architectures that can simultaneously understand and generate images (Yin et al., 2024; Yuan et al., 2025). We review this evolution and highlight the representational challenges that motivate our work.

### 2.1. Multimodal Large Language Models

**Image Understanding.** MLLM landscape has historically been divided into two primary paradigms: understanding-oriented and generation-oriented models. Understanding-oriented models excel at tasks that require interpreting visual information to produce textual outputs, such as the visual question answering task. Seminal works (Liu et al., 2023; Dai et al., 2023; Li et al., 2023b; Zhu et al., 2024), such as LLaVA (Liu et al., 2023) and MiniGPT-4 (Zhu et al., 2024), typically employ an architecture that connects a pre-trained vision encoder to a frozen LLM through a trainable interface, enabling the model to perform next-token prediction over interleaved visual and textual inputs.

**Image Generation.** Generation-oriented models, which focus on synthesizing images, have undergone a substantial architectural evolution. Earlier works were based on diffusion models (Zhang et al., 2023). These diffusion-based approaches (Rombach et al., 2022; Zhang et al., 2025; Ramesh et al., 2022; Peebles & Xie, 2023) typically formulate image synthesis as text-conditioned iterative denoising. Recent studies transition to autoregressive (AR) formulations that unify text and image generation under next-token prediction, mirroring the architecture of LLMs (Mu et al., 2025; Dong et al., 2024; Ge et al., 2024; Sun et al., 2024; Team, 2024). In AR paradigm, images are tokenized into visual sequences and concatenated with textual tokens for next-token prediction. Therefore, this unify enables simultaneous modeling of both text and images and lays the foundation for fully unified multimodal frameworks (Hang et al., 2025).

### 2.2. Unified Multimodal Large Language Models

Building on the AR paradigm, recent unified MLLMs aim to support both understanding and generation within a single architecture (Wu et al., 2025a; Deng et al., 2025; Wu et al., 2025d;c; Huang et al., 2025; Ma et al., 2025; Han et al., 2025; Wu et al., 2025b; Lin et al., 2025a; Wang et al., 2024; Xie et al., 2024; Wang et al., 2025b; Lin et al., 2025b; Chen et al., 2025a). Two major design paradigms have emerged. *Decoupled-tokenization* frameworks adopt separate visual encoders for understanding and generation, enabling each to specialize in semantic abstraction or visual synthesis, as in Janus (Wu et al., 2025a) and BAGEL (Deng et al., 2025). While this reduces cross-task interference, it leads to heavy pipelines and fragmented representation spaces. In contrast,

*shared-tokenization* frameworks aim to build a single visual space shared by understanding and generation. Representative works include VILA-U (Wu et al., 2025d), UniTok (Wu et al., 2025b) and Harmon (Wu et al., 2025c), which instantiate this idea with different architectural designs.

However, these shared-tokenization models remain largely architecture-driven, relying on heuristics such as token-text alignment (Wu et al., 2025d), masked autoregressive pre-texts (Wu et al., 2025c), or increased quantization capacity (Wu et al., 2025b). While these designs empirically improve unified modeling, they provide no explicit criterion for what shared tokens should preserve to jointly support understanding and generation. From our capacity-constrained perspective, this omission becomes more consequential because the visual tokenizer in shared-token unified MLLMs operates with finite capacity and limited computation and thus is compute-bounded. Without principled control, the allocation of representational budget between reusable structure and hard-to-exploit high-entropy variations is left largely to training dynamics. Therefore, we propose InfoTok to address this gap with IB-based objective (Tishby et al., 2000; Tishby & Zaslavsky, 2015; Alemi et al., 2017) that explicitly regulates information dependencies during tokenization.

## 3. Proposed Method

Herein, we first outline the standard unified MLLM architecture. We then introduce InfoTok and reformulate shared visual tokenization through the IB principle. Finally, we derive a tractable training objective of InfoTok via VIB.

### 3.1. Unified MLLM Frameworks

A typical unified MLLM processes multimodal inputs consisting of images  $\mathcal{I} = \{\mathcal{I}_u, \mathcal{I}_g\}$  and texts  $\mathcal{P} = \{\mathcal{P}_u, \mathcal{P}_g\}$ , where subscripts  $u$  and  $g$  denote understanding and generation respectively. A typical unified MLLM often operates through following three steps:

**1) Visual and Text Tokenization.** The shared visual encoder  $V_{enc}$  maps the input image  $\mathcal{I}$  into a sequence of visual tokens  $\mathcal{Z} = \{\mathcal{Z}_u, \mathcal{Z}_g\}$ , while a text tokenizer converts the text prompt  $\mathcal{P}$  into a sequence of text tokens  $\mathcal{T} = \{\mathcal{T}_u, \mathcal{T}_g\}$ .

**2) Multimodal Fusion.** The LLM (e.g., Qwen2.5 (Yang et al., 2024) and Ling-lite (Team et al., 2025)) receives the concatenated text and visual tokens and performs the next-token prediction. During training, the model learns to predict either the next text token  $\mathcal{M}_u$  or the next visual token  $\mathcal{M}_g$ , thereby unifying image understanding and image generation tasks within a single objective.

**3) De-Tokenization.** The predicted tokens are decoded into the target modality using a text decoder for  $\mathcal{M}_u$  and a visual decoder for  $\mathcal{M}_g$ , producing the final outputs  $\mathcal{Y} = \{\mathcal{Y}_u, \mathcal{Y}_g\}$ .

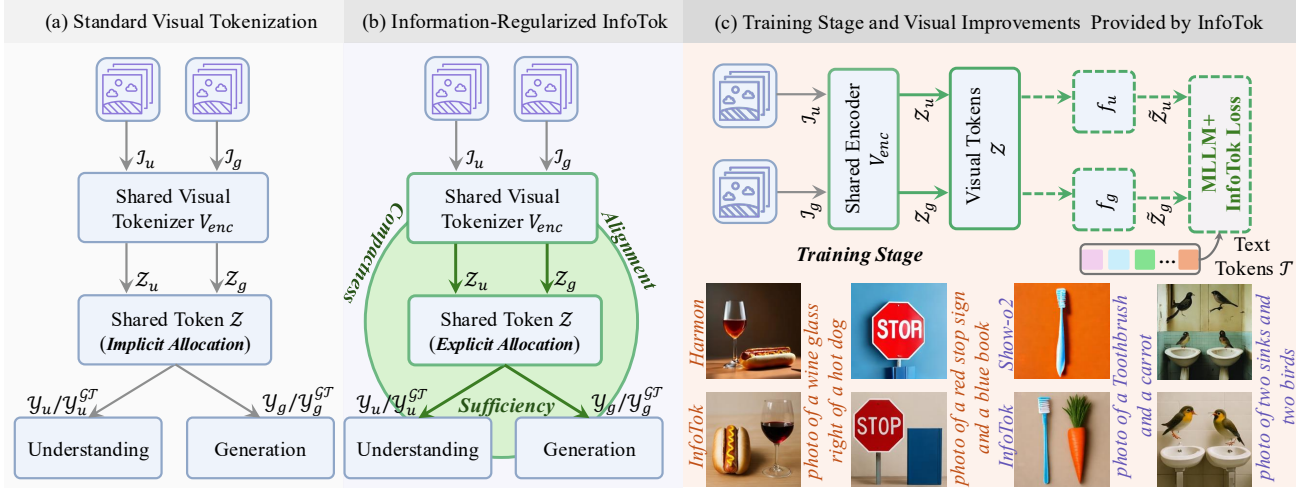


Figure 2. Illustration of our information-regularized tokenization (InfoTok). (a) depicts a standard unified MLLM with shared tokenization, where a single visual tokenizer jointly supports understanding (I2T) and generation (T2I) tasks. (b) presents InfoTok, which imposes an information-regularization objective to explicitly control what visual content is retained in the shared token space. Specifically, InfoTok promotes compact yet sufficient tokens, filtering redundant information while preserving task-critical semantics for understanding and essential perceptual cues for generation. (c) illustrates the training workflow of InfoTok. During training, the Compactness, Sufficiency, and Alignment objectives form the InfoTok loss to regularize the shared visual tokens in existing unified MLLMs. Qualitatively, after applying InfoTok to Harmon and Show-o2, we observe visibly improved instruction following and higher overall generation quality.

The training objective of a unified MLLM combines text-to-image (T2I) and image-to-text (I2T) losses:

$$\mathcal{L}_{\text{MLLM}} = \mathcal{L}_{\text{I2t}}(\mathcal{Y}_g, \mathcal{Y}_g^{\mathcal{G}\mathcal{T}}) + \mathcal{L}_{\text{t2i}}(\mathcal{Y}_u, \mathcal{Y}_u^{\mathcal{G}\mathcal{T}}), \quad (1)$$

where  $\mathcal{L}_{\text{I2t}}$  denotes a cross-entropy loss (Xie et al., 2025a; Chen et al., 2025b), and  $\mathcal{L}_{\text{t2i}}$  represents a diffusion-based reconstruction loss (Zhou et al., 2025; Deng et al., 2025). In a unified MLLM, the latent visual tokens  $\mathcal{Z}$  form the interface between the visual encoder and LLM, and thus constitute the primary channel through which visual information enters multimodal reasoning. Consequently, how  $\mathcal{Z}$  allocates representational budget between semantic structure and perceptual detail largely determines the model’s performance on both image understanding and generation.

### 3.2. Unified Information-Regularized Tokenization

#### 3.2.1. CLASSICAL IB FORMULATION

From information-theoretic perspective,  $\mathcal{Z}$  learned by a MLLM can be viewed as IB formulation (Tishby et al., 2000; Tishby & Zaslavsky, 2015). The IB framework posits that an optimal representation should capture only the information from the input that is relevant to predicting the output while discarding irrelevant information. Formally, given the input image  $\mathcal{I}$  and the target  $\mathcal{Y}^{\mathcal{G}\mathcal{T}}$ , the IB principle seeks to learn a visual latent representation  $\mathcal{Z}$  by finding the infimum of the following Lagrangian:

$$\inf_{p(\mathcal{Z}|\mathcal{I})} \mathcal{L}_{\text{IB}} \quad \text{where} \quad \mathcal{L}_{\text{IB}} = I(\mathcal{Z}; \mathcal{I}) - \beta I(\mathcal{Z}; \mathcal{Y}^{\mathcal{G}\mathcal{T}}). \quad (2)$$

Herein,  $I(\cdot; \cdot)$  denotes MI, and  $\beta \geq 0$  is the Lagrangian multiplier balancing the trade-off between information constraint  $I(\mathcal{Z}; \mathcal{I})$  and predictive sufficiency  $I(\mathcal{Z}; \mathcal{Y}^{\mathcal{G}\mathcal{T}})$ . The conditional distribution  $p(\mathcal{Z}|\mathcal{I})$  represents the mapping modeled by the shared visual encoder, describing how the latent representation  $\mathcal{Z}$  is stochastically generated from the input image  $\mathcal{I}$  under the information bottleneck formulation. It formalizes how the shared visual encoder  $V_{\text{enc}}$  mediates information retention and abstraction, acting as a probabilistic mapping from visual inputs  $\mathcal{I}$  to latent tokens  $\mathcal{Z}$ .

#### 3.2.2. EXTENDED IB FORMULATION IN INFO TOK

The IB principle provides a principled objective for learning representations that trade off compression and task relevance for a single input–output mapping. In shared-token unified MLLMs, however, a single visual tokenizer must simultaneously support two objectives, image understanding and generation, while interacting coherently with textual tokens in a unified next-token prediction pipeline. Under the unified MLLM definition in Section 3.1, the shared visual encoder  $V_{\text{enc}}$  produces visual tokens as follows:

$$\mathcal{Z}_u = V_{\text{enc}}(\mathcal{I}_u), \quad \mathcal{Z}_g = V_{\text{enc}}(\mathcal{I}_g). \quad (3)$$

To make task requirements explicit when imposing information constraints, we attach lightweight task-specific projections on top of the visual tokens (Fig. 2 (c)):

$$\tilde{\mathcal{Z}}_u = f_u(\mathcal{Z}_u), \quad \tilde{\mathcal{Z}}_g = f_g(\mathcal{Z}_g), \quad (4)$$

where  $\tilde{\mathcal{Z}}_u$  and  $\tilde{\mathcal{Z}}_g$  serve as task-facing representations used only to define the InfoTok regularization during training

*Table 1.* To verify whether InfoTok yields positive effects in unified MLLMs, we apply our information-regularized training to Harmon and Show-o2 and re-train the shared visual tokenizer  $V_{enc}$ . To assess generation, we freeze  $V_{enc}$  and train a lightweight decoder on ImageNet (Deng et al., 2009), then evaluate reconstruction quality on the ImageNet validation set using FID. To assess understanding, we measure cross-modal dependence between visual tokens and the final text representations on DenseFusion-1M (Li et al., 2024) using normalized centered kernel alignment (CKA), with 10k randomly sampled images that do not overlap with training data.

Metric	Harmon	InfoTok (Harmon)	Show-o2	InfoTok (Show-o2)
FID $\downarrow$	14.4	<b>12.0</b>	13.2	<b>11.4</b>
CKA $\uparrow$	0.24	<b>0.27</b>	0.23	<b>0.28</b>

and removed at inference. Since  $f_u$  and  $f_g$  are deterministic, constraining the information content of  $\tilde{\mathcal{Z}}$  induces corresponding pressure on the shared tokens  $\mathcal{Z}$  and thus on  $V_{enc}$ . With these task-facing tokens, InfoTok extends the classical IB objective to the shared-token setting by jointly regulating tokenization for understanding and generation, while also encouraging consistent interaction between visual and textual tokens in next-token prediction. We define the following information-regularized objectives:

$$\begin{aligned}\mathcal{L}_{IB}^{(u)} &= I(\tilde{\mathcal{Z}}_u; \mathcal{I}_u) - \beta_u I(\tilde{\mathcal{Z}}_u; \mathcal{Y}_u^{GT}) - \alpha_u I(\tilde{\mathcal{Z}}_u; \mathcal{T}_u), \\ \mathcal{L}_{IB}^{(g)} &= I(\tilde{\mathcal{Z}}_g; \mathcal{I}_g) - \beta_g I(\tilde{\mathcal{Z}}_g; \mathcal{Y}_g^{GT}) - \alpha_g I(\tilde{\mathcal{Z}}_g; \mathcal{T}_g).\end{aligned}\quad (5)$$

Here  $\alpha$  and  $\beta$  are positive Lagrange multipliers that control the trade-offs among the following objectives.

**1) Compactness:** The term  $I(\tilde{\mathcal{Z}}; \mathcal{I})$  penalizes redundant input information in the projected tokens, promoting compact representations under a limited representational budget.

**2) Sufficiency:** The term  $I(\tilde{\mathcal{Z}}; \mathcal{Y}^{GT})$  encourages the tokens to retain task-relevant information needed to predict the targets for image understanding and generation.

**3) Alignment:** The term  $I(\tilde{\mathcal{Z}}; \mathcal{T})$  encourages compatibility between visual and textual representations, reinforcing cross-modal consistency in the unified modeling pipeline.

Finally, InfoTok regularization can be defined as:

$$\mathcal{L}_{InfoTok} = \mathcal{L}_{IB}^{(u)} + \mathcal{L}_{IB}^{(g)}. \quad (6)$$

Although Eqn. (5) is written in terms of the projected tokens  $\tilde{\mathcal{Z}}_u$  and  $\tilde{\mathcal{Z}}_g$ , the resulting regularization acts on the shared encoder through the composition in Eqn. (3) and Eqn. (4). Together, these terms provide a unified mechanism for regulating information flow in shared visual tokenization  $V_{enc}$ , improving the stability of a single token space for both multimodal understanding and generation.

### 3.2.3. VARIATIONAL IB ESTIMATION IN INFO TOK

Eqn. 5 contains  $I(\tilde{\mathcal{Z}}; \mathcal{I})$ ,  $I(\tilde{\mathcal{Z}}; \mathcal{Y}^{GT})$  and  $I(\tilde{\mathcal{Z}}; \mathcal{T})$ , which are generally intractable for high-dimensional representa-

tions because the underlying joint and marginal distributions are not available in closed form (Poole et al., 2019). Thus, optimizing Eqn. 5 requires practical dependence estimators that are differentiable during training. In this paper, InfoTok can be instantiated with feasible VIB estimators that serve this role (Alemi et al., 2017). Following Eqn. 3 and Eqn. 4, we model tokenization with a variational posterior  $q_\phi(\tilde{\mathcal{Z}} \mid \mathcal{I})$ . Specifically,  $q_\phi(\tilde{\mathcal{Z}} \mid \mathcal{I})$  is parameterized as a Gaussian with mean  $\mu_\phi(\mathcal{I})$  and variance  $\sigma_\phi^2(\mathcal{I})$ , and  $\tilde{\mathcal{Z}}$  is sampled via the reparameterization trick from  $\mathcal{N}(\mu_\phi(\mathcal{I}), \text{diag}(\sigma_\phi^2(\mathcal{I})))$  (Kingma & Welling, 2014). This probabilistic relaxation yields tractable surrogates for the three components shown in Eqn. 5.

**1) Compactness Term.** We upper bound  $I(\tilde{\mathcal{Z}}; \mathcal{I})$  by KL divergence between the variational posterior and a prior, yielding the standard VIB bounds:

$$\begin{aligned}I(\tilde{\mathcal{Z}}_u; \mathcal{I}_u) &\leq \mathbb{E}_{p(\mathcal{I}_u)} \left[ D_{KL}(q_\phi(\tilde{\mathcal{Z}}_u \mid \mathcal{I}_u) \parallel r_u(\tilde{\mathcal{Z}}_u)) \right], \\ I(\tilde{\mathcal{Z}}_g; \mathcal{I}_g) &\leq \mathbb{E}_{p(\mathcal{I}_g)} \left[ D_{KL}(q_\phi(\tilde{\mathcal{Z}}_g \mid \mathcal{I}_g) \parallel r_g(\tilde{\mathcal{Z}}_g)) \right],\end{aligned}\quad (7)$$

where  $r_u(\tilde{\mathcal{Z}}_u)$  and  $r_g(\tilde{\mathcal{Z}}_g)$  are priors, typically  $\mathcal{N}(0, \mathbf{I}_d)$ . Minimizing these KL terms encourages compact projected tokens by suppressing redundant input information.

**2) Sufficiency Term.** To ensure the projected tokens remain predictive of task targets, we lower bound  $I(\tilde{\mathcal{Z}}; \mathcal{Y}^{GT})$  with variational decoders  $p_\theta(\mathcal{Y}_u^{GT} \mid \tilde{\mathcal{Z}}_u)$  and  $p_\theta(\mathcal{Y}_g^{GT} \mid \tilde{\mathcal{Z}}_g)$ :

$$\begin{aligned}I(\tilde{\mathcal{Z}}_u; \mathcal{Y}_u^{GT}) &\geq \mathbb{E}_{p(\mathcal{I}_u, \mathcal{Y}_u^{GT})} \left[ \log p_\theta(\mathcal{Y}_u^{GT} \mid \tilde{\mathcal{Z}}_u) \right] + H(\mathcal{Y}_u^{GT}), \\ I(\tilde{\mathcal{Z}}_g; \mathcal{Y}_g^{GT}) &\geq \mathbb{E}_{p(\mathcal{I}_g, \mathcal{Y}_g^{GT})} \left[ \log p_\theta(\mathcal{Y}_g^{GT} \mid \tilde{\mathcal{Z}}_g) \right] + H(\mathcal{Y}_g^{GT}),\end{aligned}\quad (8)$$

where  $H(\mathcal{Y}^{GT})$  is the entropy of the target and remains constant during the model optimization.

**3) Alignment Term.** To encourage coherent interaction with text, we maximize  $I(\tilde{\mathcal{Z}}; \mathcal{T})$  using a contrastive estimator. For each branch, we aggregate a visual embedding from the posterior mean,  $\tilde{\mathcal{Z}}_u = \text{mean}(\mu_\phi(\mathcal{I}_u))$  and  $\tilde{\mathcal{Z}}_g = \text{mean}(\mu_\phi(\mathcal{I}_g))$ , and apply an InfoNCE-based estimator (van den Oord et al., 2018) defined as:

$$\begin{aligned}\hat{I}(\tilde{\mathcal{Z}}_u; \mathcal{T}_u) &= \mathbb{E} \left[ \log \frac{\exp(\text{sim}(\tilde{\mathcal{Z}}_u, \mathcal{T}_u)/\tau)}{\sum_k \exp(\text{sim}(\tilde{\mathcal{Z}}_u, \mathcal{T}_{u,k})/\tau)} \right], \\ \hat{I}(\tilde{\mathcal{Z}}_g; \mathcal{T}_g) &= \mathbb{E} \left[ \log \frac{\exp(\text{sim}(\tilde{\mathcal{Z}}_g, \mathcal{T}_g)/\tau)}{\sum_k \exp(\text{sim}(\tilde{\mathcal{Z}}_g, \mathcal{T}_{g,k})/\tau)} \right],\end{aligned}\quad (9)$$

where  $\text{sim}(\cdot, \cdot)$  is cosine similarity,  $\tau$  is a temperature parameter, and  $\mathcal{T}_{u,k}$  and  $\mathcal{T}_{g,k}$  are negative textual samples.

**Final Objective.** Combining the compactness upper bound and the sufficiency and alignment lower bounds yields a unified differentiable surrogate for Eqn. 5:

Table 2. Comparison of unified MLLMs on Geneval and WISE benchmarks. Gray-shaded InfoTok rows show absolute improvements. **Boldface** values indicate that, after InfoTok regularization, the performance ranks within the top three among all compared methods.

Model	Year	Size	Single Obj.	Color Attr.	Colors	Position	Counting	Two Obj.	Overall	WISE
Show-o2	2025	7.0B	0.98	0.48	0.83	0.25	0.49	0.80	0.64	0.40
Ovis-U1	2025	3.6B	1.00	0.77	0.91	0.80	0.86	0.98	0.89	0.48
Janus	2025	1.3B	0.94	0.45	0.82	0.50	0.31	0.66	0.61	0.31
Janus-Pro	2025	1.0B	0.96	0.54	0.87	0.50	0.44	0.70	0.67	0.25
Show-o	2025	1.5B	0.97	0.81	0.30	0.68	0.82	0.51	0.68	0.43
Harmon	2025	1.5B	0.99	0.51	0.86	0.49	0.73	0.88	0.74	0.45
InfoTok (Harmon)	2025	1.5B	<b>1.00<sup>+0.01</sup></b>	0.73 <sup>+0.22</sup>	<b>0.91<sup>+0.05</sup></b>	<b>0.78<sup>+0.29</sup></b>	<b>0.76<sup>+0.03</sup></b>	<b>0.94<sup>+0.06</sup></b>	<b>0.85<sup>+0.11</sup></b>	<b>0.60<sup>+0.15</sup></b>
OpenUni	2025	2.0B	0.99	0.72	0.89	0.77	0.74	0.91	0.84	0.55
InfoTok (OpenUni)	2025	2.0B	<b>0.99<sup>+0.00</sup></b>	<b>0.74<sup>+0.02</sup></b>	<b>0.89<sup>+0.00</sup></b>	<b>0.80<sup>+0.03</sup></b>	<b>0.74<sup>+0.00</sup></b>	<b>0.92<sup>+0.01</sup></b>	<b>0.85<sup>+0.01</sup></b>	<b>0.58<sup>+0.03</sup></b>
Show-o2	2025	1.5B	0.98	0.43	0.79	0.24	0.45	0.72	0.60	0.39
InfoTok (Show-o2)	2025	1.5B	<b>0.99<sup>+0.01</sup></b>	0.60 <sup>+0.17</sup>	0.84 <sup>+0.05</sup>	0.50 <sup>+0.26</sup>	0.52 <sup>+0.07</sup>	0.82 <sup>+0.10</sup>	<b>0.71<sup>+0.11</sup></b>	0.43 <sup>+0.04</sup>

$$\begin{aligned}
\mathcal{L}_{\text{InfoTok}}^{(u)} &= \mathbb{E}_{p(\mathcal{I}_u)} [D_{\text{KL}}(q_\phi(\tilde{\mathcal{Z}}_u | \mathcal{I}_u) \| r_u(\tilde{\mathcal{Z}}_u))] \\
&\quad - \beta_u \mathbb{E}_{p(\mathcal{I}_u, \mathcal{Y}_u^{\mathcal{G}\mathcal{T}})} [\log p_\theta(\mathcal{Y}_u^{\mathcal{G}\mathcal{T}} | \tilde{\mathcal{Z}}_u)] - \alpha_u \hat{I}(\tilde{\mathcal{Z}}_u; \mathcal{T}_u), \\
\mathcal{L}_{\text{InfoTok}}^{(g)} &= \mathbb{E}_{p(\mathcal{I}_g)} [D_{\text{KL}}(q_\phi(\tilde{\mathcal{Z}}_g | \mathcal{I}_g) \| r_g(\tilde{\mathcal{Z}}_g))] \\
&\quad - \beta_g \mathbb{E}_{p(\mathcal{I}_g, \mathcal{Y}_g^{\mathcal{G}\mathcal{T}})} [\log p_\theta(\mathcal{Y}_g^{\mathcal{G}\mathcal{T}} | \tilde{\mathcal{Z}}_g)] - \alpha_g \hat{I}(\tilde{\mathcal{Z}}_g; \mathcal{T}_g), \\
\mathcal{L}_{\text{InfoTok}} &= \mathcal{L}_{\text{InfoTok}}^{(u)} + \mathcal{L}_{\text{InfoTok}}^{(g)}. \tag{10}
\end{aligned}$$

### 3.3. Training Objective and Theoretical Grounding

#### 3.3.1. TRAINING OBJECTIVE

InfoTok is implemented as a fine-tuning stage for pretrained unified MLLMs. As shown in Fig. 2 (c), we optimize the original multimodal task objective together with the proposed information regularization. A key implementation detail is that the information constraints in Eqn. 5 are instantiated on the projected tokens  $\tilde{\mathcal{Z}}$ , since  $\tilde{\mathcal{Z}}$  is the task-facing representation used to define the compactness, sufficiency, and alignment estimators in Section 3.2. During training, InfoTok therefore provides direct supervision on  $\tilde{\mathcal{Z}}$ . This supervision propagates through the task-specific projections and indirectly regulates the encoder tokens  $\mathcal{Z}$  and the shared visual encoder  $V_{\text{enc}}$  via Eqn. 3 and Eqn. 4. Finally, the overall training objective can be defined as:

$$\mathcal{L}_{\text{Total}} = \mathcal{L}_{\text{MLLM}} + \lambda \mathcal{L}_{\text{InfoTok}}. \tag{11}$$

$\lambda$  balances task optimization and information regularization. Minimizing  $\mathcal{L}_{\text{Total}}$  fine-tunes the  $V_{\text{enc}}$  to learn visual tokens that remain compact, task-relevant, and cross-modally consistent for both understanding and generation. In Tab. 1 and Tab. 2, we can see that InfoTok effectively improves model’s tokenization and boosts overall performance.

#### 3.3.2. THEORETICAL GROUNDING

Beyond empirical gains, we provide a theoretical rationale for why a shared visual tokenizer can remain information-

sufficient for both understanding and generation. In unified MLLMs, the LLM consumes encoder tokens produced by the shared visual encoder  $V_{\text{enc}}$ . During training, we optionally introduce lightweight task-specific projections to expose task requirements when constructing InfoTok regularization, namely  $\mathcal{Z}_u = V_{\text{enc}}(\mathcal{I}_u)$ ,  $\mathcal{Z}_g = V_{\text{enc}}(\mathcal{I}_g)$  and  $\tilde{\mathcal{Z}}_u = f_u(\mathcal{Z}_u)$ ,  $\tilde{\mathcal{Z}}_g = f_g(\mathcal{Z}_g)$ . Since  $f_u$  and  $f_g$  are deterministic post-processing, we can derive that:

$$I(\mathcal{Z}; \mathcal{Y}^{\mathcal{G}\mathcal{T}}) \geq \max(I(\tilde{\mathcal{Z}}_u; \mathcal{Y}_u^{\mathcal{G}\mathcal{T}}), I(\tilde{\mathcal{Z}}_g; \mathcal{Y}_g^{\mathcal{G}\mathcal{T}})), \tag{12}$$

which shows that regularizing the task-facing tokens  $\tilde{\mathcal{Z}}$  induces corresponding information constraints on the shared encoder outputs  $\mathcal{Z}$ . The projections are used only during training and removed at inference, while the shared encoder inherits the resulting pressure. Although deterministic processing cannot increase mutual information, it can reshape the representation into a form that is more exploitable by the multimodal predictor, which motivates using InfoTok as a unified regularizer across understanding and generation.

## 4. Experiment

### 4.1. Experiment Setup

**Experiment Details.** We evaluate InfoTok on three shared-tokenization unified MLLMs, namely Show-o2 (Xie et al., 2025b), OpenUni (Wu et al., 2025b) and Harmon (Wu et al., 2025c), to verify its effectiveness as a plug-and-play regularization module. For each baseline, we start from the officially released checkpoints and fine-tune with InfoTok using the same training data as baseline (approximately 1.5M paired I2T and T2I sub-samples) without introducing additional data. All experiments are conducted on 16 NVIDIA L40S-48G GPUs. The training and architectural configurations strictly follow the original implementations, and the initial learning rate is set to one tenth of the original to ensure stable adaptation. This controlled setup ensures that any observed improvement originates from InfoTok.

Table 3. Comparison on the Geneval++ dataset. Gray-shaded InfoTok rows show absolute improvements. **Boldface** values indicate that, after InfoTok regularization, the performance ranks within the top three among all compared methods.

Model	Year	Size	Color	Spa_Cou.	Color_Spa.	Color_Cou.	Multi_Obj.	Size_Spa.	Counting	Overall
Show-o2	2025	7.0B	0.25	0.08	0.28	0.10	0.18	0.25	0.10	0.18
Ovis-U1	2025	3.6B	0.48	0.33	0.53	0.38	0.43	0.58	0.45	0.45
Janus	2025	1.3B	0.08	0.03	0.10	0.10	0.08	0.05	0.23	0.10
Janus-Pro	2025	1.0B	0.28	0.05	0.20	0.03	0.05	0.18	0.20	0.14
Show-o	2025	1.5B	0.30	0.10	0.33	0.18	0.23	0.18	0.43	0.25
Harmon	2025	1.5B	0.30	0.03	0.10	0.15	0.18	0.18	0.38	0.19
InfoTok (Harmon)	2025	1.5B	<b>0.58<sup>+0.28</sup></b>	<b>0.15<sup>+0.12</sup></b>	<b>0.53<sup>+0.43</sup></b>	<b>0.40<sup>+0.25</sup></b>	<b>0.50<sup>+0.32</sup></b>	<b>0.45<sup>+0.27</sup></b>	<b>0.60<sup>+0.22</sup></b>	<b>0.46<sup>+0.27</sup></b>
OpenUni	2025	2.0B	0.45	0.23	0.48	0.45	0.30	0.50	0.50	0.42
InfoTok (OpenUni)	2025	2.0B	<b>0.53<sup>+0.08</sup></b>	<b>0.23<sup>+0.00</sup></b>	<b>0.60<sup>+0.12</sup></b>	<b>0.45<sup>+0.00</sup></b>	<b>0.38<sup>+0.08</sup></b>	<b>0.55<sup>+0.05</sup></b>	<b>0.50<sup>+0.00</sup></b>	<b>0.46<sup>+0.04</sup></b>
Show-o2	2025	1.5B	0.28	0.03	0.20	0.10	0.15	0.28	0.18	0.17
InfoTok (Show-o2)	2025	1.5B	<b>0.39<sup>+0.11</sup></b>	<b>0.10<sup>+0.07</sup></b>	<b>0.30<sup>+0.10</sup></b>	<b>0.22<sup>+0.12</sup></b>	<b>0.24<sup>+0.09</sup></b>	<b>0.39<sup>+0.11</sup></b>	<b>0.28<sup>+0.10</sup></b>	<b>0.27<sup>+0.10</sup></b>

**Evaluation Datasets.** Following existing works, we conduct experiments on ten representative datasets covering both understanding and generation tasks. Specifically, we evaluate understanding performance on six widely used benchmarks: GQA (Hudson & Manning, 2019), SEED (Li et al., 2023a), POPE (Li et al., 2023c), MME (Fu et al., 2023), MMV2 (Yu et al., 2024) and MMMU (Yue et al., 2024). For generation evaluation, we employ three standard benchmarks: Geneval (Ghosh et al., 2023), Geneval++ (Ye et al., 2025), and WISE (Niu et al., 2025). To further assess the unified multimodal capability of each model, we include UniBench (Li et al., 2025) dataset, which jointly evaluates image understanding and generation in a single pipeline.

**Comparison Methods.** To further illustrate the performance level InfoTok can achieve, we compare our InfoTok fine-tuned variants with several strong open-source models of similar or slightly larger scale, including Janus-1.3B (Wu et al., 2025a), Janus-Pro-1B (Chen et al., 2025b), and Show-o (Xie et al., 2025a). Larger models such as Ovis-U1-3.6B (Wang et al., 2025a) and Show-o2-7B (Xie et al., 2025b) are also included as references for full comparison. These comparisons show that incorporating our proposed InfoTok can significantly enhance the performance of smaller-scale models, allowing them to achieve results comparable to or even surpassing larger unified MLLMs.

## 4.2. Analysis of Experimental Results

### Analysis 1: Overall Effectiveness of InfoTok

As shown in Tabs. 2, 3, and 4, InfoTok yields consistent gains on both generation and understanding benchmarks across all evaluated unified MLLMs. These results support our purpose: IB-regularized tokenization promotes compact yet sufficient visual tokens by prioritizing reusable structure and suppressing redundant high-entropy variations. **Therefore, instead of engineering more complex tokenizers, our proposed InfoTok improves unified MLLMs by explicitly regulating the information flow in visual tokenization.**

### Analysis 2: Effects across Different Architectures

We further study how InfoTok behaves across unified MLLMs with different multimodal-fusion paradigms. OpenUni (Wu et al., 2025b) builds on a frozen VLM backbone (e.g., InternVL3 (Zhu et al., 2025)) and is fine-tuned mainly for generation. In contrast, the second category, including Harmon (Wu et al., 2025c) and Show-o2 (Xie et al., 2025b), employs trainable LLM (e.g., Qwen2.5 (Yang et al., 2024)) as their multimodal fusion core, which jointly optimizes understanding and generation through unified tokenization. As shown in Tabs. 2, 3, and 4, InfoTok yields smaller gains on OpenUni but delivers substantial and consistent improvements on Harmon and Show-o2. This trend shows that InfoTok is most effective when the shared visual tokenizer is shaped by gradients from both understanding and generation, enabling IB regularization to allocate representational budget toward reusable structure rather than high-entropy variations. By contrast, when training signals are dominated by generation-only objectives, tokens tend to emphasize appearance cues and leave less room for InfoTok to improve semantic abstraction and cross-modal reasoning. **Overall, InfoTok favors architectures with fully trainable multimodal fusion, where understanding and generation can genuinely co-shape a shared token space.**

### Analysis 3: Effects across Different Visual Encoders

We also examine InfoTok under different visual encoding paradigms. Harmon uses a continuous visual encoder, whereas Show-o2 adopts a discrete tokenizer. As shown in Tabs. 2, 3, and 4, InfoTok improves both models but with different emphases: it tends to benefit Harmon more on generation and Show-o2 more on understanding. This aligns with their representational biases. Harmon’s continuous tokens are expressive but often redundant, so InfoTok mainly strengthens generation by enforcing compact yet sufficient structure. Show-o2’s quantized tokens are naturally suited for synthesis but can under-represent semantics; InfoTok enhances semantic sufficiency and visual–text alignment, leading to a larger average understanding gain. **Overall, these**

Table 4. Comparison with recent unified MLLMs on image understanding benchmarks. Gray-shaded rows show absolute improvements. **Boldface** values indicate that, after InfoTok regularization, the performance ranks within the top three among all compared methods.

Model	Year	Size	MME	POPE	SEED	GQA	MMMU	MMV2	UniBench
Show-o2	2025	7.0B	2021	0.85	0.75	0.66	0.47	0.37	0.69
Ovis-U1	2025	3.6B	2040	0.89	0.76	0.59	0.30	0.55	0.62
Janus	2025	1.3B	1107	0.57	0.64	0.49	0.29	0.27	0.55
Janus-Pro	2025	1.0B	1739	0.83	0.65	0.58	0.29	0.31	0.52
Show-o	2025	1.5B	1216	0.82	0.57	0.57	0.24	0.18	0.39
Harmon	2025	1.5B	1411	0.76	0.65	0.51	0.36	0.25	0.64
InfoTok (Harmon)	2025	1.5B	1548 <sup>+137</sup>	<b>0.84<sup>+0.08</sup></b>	<b>0.66<sup>+0.01</sup></b>	<b>0.59<sup>+0.08</sup></b>	<b>0.37<sup>+0.01</sup></b>	0.27 <sup>+0.02</sup>	<b>0.66<sup>+0.02</sup></b>
Show-o2	2025	1.5B	1714	0.84	0.66	0.58	0.36	0.28	0.39
InfoTok (Show-o2)	2025	1.5B	1823 <sup>+109</sup>	<b>0.85<sup>+0.01</sup></b>	<b>0.69<sup>+0.03</sup></b>	<b>0.61<sup>+0.03</sup></b>	<b>0.37<sup>+0.01</sup></b>	0.30 <sup>+0.02</sup>	0.49 <sup>+0.10</sup>

Table 5. Ablation results on Harmon and Show-o2 under identical data budgets (subsets sampled from each baseline’s original training set). We compare standard fine-tuning with InfoTok-regularized fine-tuning, and further ablate the three components in InfoTok: Compactness (C) and Sufficiency (S), which are the canonical terms in the IB objective, and Alignment (A), our extended cross-modal term.

Model	MME	POPE	SEED	GQA	MMMU	MMV2	UniBench	WISE	Geneval	Geneval++
Harmon	1411	0.76	0.65	0.51	0.36	0.25	0.64	0.45	0.74	0.19
Finetune	1405 <sup>+006</sup>	0.78 <sup>+0.02</sup>	0.64 <sup>-0.01</sup>	0.51 <sup>+000</sup>	0.34 <sup>-0.02</sup>	0.26 <sup>+0.01</sup>	0.62 <sup>-0.02</sup>	0.46 <sup>+0.01</sup>	0.72 <sup>-0.02</sup>	0.17 <sup>-0.02</sup>
InfoTok (C&S)	1503 <sup>+092</sup>	0.82 <sup>+0.06</sup>	0.66 <sup>+0.01</sup>	0.55 <sup>+0.04</sup>	0.37 <sup>+0.01</sup>	0.27 <sup>+0.02</sup>	0.66 <sup>+0.02</sup>	0.60 <sup>+0.15</sup>	0.84 <sup>+0.10</sup>	0.43 <sup>+0.24</sup>
InfoTok (C&S&A)	<b>1548<sup>+137</sup></b>	<b>0.84<sup>+0.08</sup></b>	<b>0.66<sup>+0.01</sup></b>	<b>0.59<sup>+0.08</sup></b>	<b>0.37<sup>+0.01</sup></b>	<b>0.27<sup>+0.02</sup></b>	<b>0.66<sup>+0.02</sup></b>	<b>0.60<sup>+0.15</sup></b>	<b>0.85<sup>+0.11</sup></b>	<b>0.46<sup>+0.27</sup></b>
Show-o2	1714	0.84	0.66	0.58	0.36	0.28	0.39	0.39	0.60	0.17
Finetune	1738 <sup>+024</sup>	0.83 <sup>-0.01</sup>	0.65 <sup>-0.01</sup>	0.58 <sup>+0.00</sup>	0.35 <sup>-0.01</sup>	0.29 <sup>+0.01</sup>	0.40 <sup>+0.01</sup>	0.41 <sup>+0.02</sup>	0.60 <sup>+0.00</sup>	0.18 <sup>+0.01</sup>
InfoTok (C&S)	1801 <sup>+087</sup>	0.85 <sup>+0.01</sup>	0.68 <sup>+0.02</sup>	0.59 <sup>+0.01</sup>	0.37 <sup>+0.01</sup>	0.30 <sup>+0.02</sup>	0.46 <sup>+0.07</sup>	0.42 <sup>+0.03</sup>	0.67 <sup>+0.07</sup>	0.25 <sup>+0.08</sup>
InfoTok (C&S&A)	<b>1823<sup>+109</sup></b>	<b>0.85<sup>+0.01</sup></b>	<b>0.69<sup>+0.03</sup></b>	<b>0.61<sup>+0.03</sup></b>	<b>0.37<sup>+0.01</sup></b>	<b>0.30<sup>+0.02</sup></b>	<b>0.49<sup>+0.10</sup></b>	<b>0.43<sup>+0.04</sup></b>	<b>0.71<sup>+0.11</sup></b>	<b>0.27<sup>+0.10</sup></b>

**results support our thesis that information-regularized tokenization offers a more general lever for unification than architecture-specific tokenizer redesign.**

### 4.3. Ablation Studies

According to **Analysis 2**, OpenUni adopts a frozen VLM-based fusion backbone and is primarily optimized for generation, making it less suitable for probing how a shared tokenizer jointly supports understanding and generation. Therefore, we conduct ablations on Harmon and Show-o2, two representative shared-token unified MLLMs with fully trainable tokenization and fusion, to isolate the impact of InfoTok on both capability dimensions.

Tab. 5 compares the original models, standard fine-tuning, and InfoTok-regularized fine-tuning under the same fine-tuning data. Across both understanding benchmarks and generation benchmarks, InfoTok consistently yields clear improvements. In contrast, standard fine-tuning leads to only marginal and sometimes oscillatory changes across datasets, failing to provide reliable gains and occasionally degrading performance. This gap indicates that naive fine-tuning does not effectively improve shared tokenization under a limited representational budget, whereas InfoTok provides an explicit information-regularized objective that reshapes  $V_{enc}$  toward more compact yet sufficient tokens.

Notably, Tab. 5 shows that using only the canonical IB terms, Compactness and Sufficiency, already yields clear and consistent improvements over both Harmon and Show-o2. This suggests that the core benefit of InfoTok comes from explicitly regulating the compression-relevance trade-off during token formation, rather than relying on implicit optimization. When we further include the Alignment term, performance typically improves or becomes more stable across benchmarks, indicating that visual-text coupling benefits the unified next-token prediction.

## 5. Conclusion

We proposed InfoTok, an IB grounded framework for information-regularized visual tokenization in shared-token unified MLLMs. Motivated by a capacity-constrained view, InfoTok explicitly regulates what shared tokens preserve under a limited representational budget via a tractable variational formulation. Experiments on representative unified MLLMs show consistent improvements on both understanding and generation without additional data or architectural changes. We hope this work provides insight into how information-theoretic principles can be practically applied to enhance multimodal learning and inspire future research on unified and interpretable multimodal representations.

## Impact Statements

This paper presents work whose goal is to advance the field of machine learning. There are many potential societal consequences of our work, none of which we feel must be specifically highlighted here.

## References

Alemi, A. A., Fischer, I., Dillon, J. V., and Murphy, K. Deep variational information bottleneck. In *ICLR*. OpenReview.net, 2017.

Chen, J., Xu, Z., Pan, X., Hu, Y., Qin, C., Goldstein, T., Huang, L., Zhou, T., Xie, S., Savarese, S., Xue, L., Xiong, C., and Xu, R. Blip3-o: A family of fully open unified multimodal models-architecture, training and dataset. *CoRR*, abs/2505.09568, 2025a.

Chen, X., Wu, Z., Liu, X., Pan, Z., Liu, W., Xie, Z., Yu, X., and Ruan, C. Janus-pro: Unified multimodal understanding and generation with data and model scaling. *CoRR*, abs/2501.17811, 2025b.

Dai, W., Li, J., Li, D., Tiong, A. M. H., Zhao, J., Wang, W., Li, B., Fung, P., and Hoi, S. C. H. Instructblip: Towards general-purpose vision-language models with instruction tuning. In *NeurIPS*, 2023.

Deng, C., Zhu, D., Li, K., Gou, C., Li, F., Wang, Z., Zhong, S., Yu, W., Nie, X., Song, Z., Guang, S., and Fan, H. Emerging properties in unified multimodal pretraining. *CoRR*, abs/2505.14683, 2025.

Deng, J., Dong, W., Socher, R., Li, L., Li, K., and Fei-Fei, L. Imagenet: A large-scale hierarchical image database. In *CVPR*, pp. 248–255. IEEE Computer Society, 2009.

Dong, R., Han, C., Peng, Y., Qi, Z., Ge, Z., Yang, J., Zhao, L., Sun, J., Zhou, H., Wei, H., Kong, X., Zhang, X., Ma, K., and Yi, L. Dreamllm: Synergistic multimodal comprehension and creation. In *ICLR*. OpenReview.net, 2024.

Fu, C., Chen, P., Shen, Y., Qin, Y., Zhang, M., Lin, X., Qiu, Z., Lin, W., Yang, J., Zheng, X., Li, K., Sun, X., and Ji, R. MME: A comprehensive evaluation benchmark for multimodal large language models. *CoRR*, abs/2306.13394, 2023.

Ge, Y., Zhao, S., Zeng, Z., Ge, Y., Li, C., Wang, X., and Shan, Y. Making llama SEE and draw with SEED tokenizer. In *ICLR*. OpenReview.net, 2024.

Ghosh, D., Hajishirzi, H., and Schmidt, L. Geneval: An object-focused framework for evaluating text-to-image alignment. In *NeurIPS*, 2023.

Han, J., Chen, H., Zhao, Y., Wang, H., Zhao, Q., Yang, Z., He, H., Yue, X., and Jiang, L. Vision as a dialect: Unifying visual understanding and generation via text-aligned representations. *CoRR*, abs/2506.18898, 2025.

Hang, T., Bao, J., Wei, F., and Chen, D. Fast autoregressive models for continuous latent generation. *CoRR*, abs/2504.18391, 2025.

Huang, Z., Zheng, D., Zou, C., Liu, R., Wang, X., Ji, K., Chai, W., Sun, J., Wang, L., Lv, Y., et al. Ming-univision: Joint image understanding and generation with a unified continuous tokenizer. *CoRR*, abs/2510.06590, 2025.

Hudson, D. A. and Manning, C. D. GQA: A new dataset for real-world visual reasoning and compositional question answering. In *CVPR*, pp. 6700–6709. IEEE, 2019.

Kingma, D. P. and Welling, M. Auto-encoding variational bayes. In Bengio, Y. and LeCun, Y. (eds.), *ICLR*, 2014.

Li, B., Wang, R., Wang, G., Ge, Y., Ge, Y., and Shan, Y. Seed-bench: Benchmarking multimodal llms with generative comprehension. *CoRR*, abs/2307.16125, 2023a.

Li, J., Li, D., Savarese, S., and Hoi, S. C. H. BLIP-2: bootstrapping language-image pre-training with frozen image encoders and large language models. In *ICML*, volume 202 of *Proceedings of Machine Learning Research*, pp. 19730–19742. PMLR, 2023b.

Li, X., Zhang, F., Diao, H., Wang, Y., Wang, X., and Duan, L. Densefusion-1m: Merging vision experts for comprehensive multimodal perception. *NeurIPS*, pp. 18535–18556, 2024.

Li, Y., Du, Y., Zhou, K., Wang, J., Zhao, W. X., and Wen, J. Evaluating object hallucination in large vision-language models. In *EMNLP*, pp. 292–305. Association for Computational Linguistics, 2023c.

Li, Y., Wang, H., Zhang, Q., Xiao, B., Hu, C., Wang, H., and Li, X. Unieval: Unified holistic evaluation for unified multimodal understanding and generation. *CoRR*, abs/2505.10483, 2025.

Lin, B., Li, Z., Cheng, X., Niu, Y., Ye, Y., He, X., Yuan, S., Yu, W., Wang, S., Ge, Y., Pang, Y., and Yuan, L. Uniworld-v1: High-resolution semantic encoders for unified visual understanding and generation. *CoRR*, abs/2506.03147, 2025a.

Lin, H., Wang, T., Ge, Y., Ge, Y., Lu, Z., Wei, Y., Zhang, Q., Sun, Z., and Shan, Y. Toklip: Marry visual tokens to CLIP for multimodal comprehension and generation. *CoRR*, abs/2505.05422, 2025b.

Liu, H., Li, C., Wu, Q., and Lee, Y. J. Visual instruction tuning. In *NeurIPS*, 2023.

Ma, C., Jiang, Y., Wu, J., Yang, J., Yu, X., Yuan, Z., Peng, B., and Qi, X. Unitok: A unified tokenizer for visual generation and understanding. *CoRR*, abs/2502.20321, 2025.

Mu, J., Vasconcelos, N., and Wang, X. Editar: Unified conditional generation with autoregressive models. In *CVPR*, pp. 7899–7909. IEEE, 2025.

Niu, Y., Ning, M., Zheng, M., Lin, B., Jin, P., Liao, J., Ning, K., Zhu, B., and Yuan, L. WISE: A world knowledge-informed semantic evaluation for text-to-image generation. *CoRR*, abs/2503.07265, 2025.

Peebles, W. and Xie, S. Scalable diffusion models with transformers. In *ICCV*, pp. 4172–4182. IEEE, 2023.

Poole, B., Ozair, S., van den Oord, A., Alemi, A. A., and Tucker, G. On variational bounds of mutual information. In *ICML*, volume 97 of *Proceedings of Machine Learning Research*, pp. 5171–5180. PMLR, 2019.

Ramesh, A., Dhariwal, P., Nichol, A., Chu, C., and Chen, M. Hierarchical text-conditional image generation with CLIP latents. *CoRR*, abs/2204.06125, 2022.

Rombach, R., Blattmann, A., Lorenz, D., Esser, P., and Ommer, B. High-resolution image synthesis with latent diffusion models. In *CVPR*, pp. 10674–10685. IEEE, 2022.

Sun, Q., Cui, Y., Zhang, X., Zhang, F., Yu, Q., Wang, Y., Rao, Y., Liu, J., Huang, T., and Wang, X. Generative multimodal models are in-context learners. In *CVPR*, pp. 14398–14409. IEEE, 2024.

Team, C. Chameleon: Mixed-modal early-fusion foundation models. *CoRR*, abs/2405.09818, 2024.

Team, L., Zeng, B., Huang, C., Zhang, C., Tian, C., Chen, C., Jin, D., Yu, F., Zhu, F., Yuan, F., Wang, F., Wang, G., Zhai, G., Zhang, H., Li, H., Zhou, J., Liu, J., Fang, J., Ou, J., Hu, J., Luo, J., Zhang, J., Liu, J., Sha, J., Qian, J., Wu, J., Zhao, J., Li, J., Feng, J., Di, J., Xu, J., Yao, J., Xu, K., Du, K., Li, L., Liang, L., Yu, L., Tang, L., Ju, L., Xu, P., Cui, Q., Liu, S., Li, S., Song, S., Yan, S., Cai, T., Chen, T., Guo, T., Huang, T., Feng, T., Wu, T., Wu, W., Zhang, X., Yang, X., Zhao, X., Hu, X., Lin, X., Zhao, Y., Wang, Y., Guo, Y., Wang, Y., Yang, Y., Cao, Y., Fu, Y., Xiong, Y., Li, Y., Li, Z., Zhang, Z., Liu, Z., Huan, Z., Wen, Z., Sun, Z., Du, Z., and He, Z. Every FLOP counts: Scaling a 300b mixture-of-experts LING LLM without premium gpus. *CoRR*, abs/2503.05139, 2025.

Tishby, N. and Zaslavsky, N. Deep learning and the information bottleneck principle. In *ITW*, pp. 1–5. IEEE, 2015.

Tishby, N., Pereira, F. C. N., and Bialek, W. The information bottleneck method. *CoRR*, physics/0004057, 2000.

van den Oord, A., Li, Y., and Vinyals, O. Representation learning with contrastive predictive coding. *CoRR*, abs/1807.03748, 2018.

Wang, G., Zhao, S., Zhang, X., Cao, L., Zhan, P., Duan, L., Lu, S., Fu, M., Chen, X., Zhao, J., Li, Y., and Chen, Q. Ovis-ul technical report. *CoRR*, abs/2506.23044, 2025a.

Wang, H., Han, J., Yang, Z., Zhao, Q., Lin, S., Yue, X., Shrivastava, A., Yang, Z., and Chen, H. Growing visual generative capacity for pre-trained mllms. *CoRR*, abs/2510.01546, 2025b.

Wang, X., Zhang, X., Luo, Z., Sun, Q., Cui, Y., Wang, J., Zhang, F., Wang, Y., Li, Z., Yu, Q., Zhao, Y., Ao, Y., Min, X., Li, T., Wu, B., Zhao, B., Zhang, B., Wang, L., Liu, G., He, Z., Yang, X., Liu, J., Lin, Y., Huang, T., and Wang, Z. Emu3: Next-token prediction is all you need. *CoRR*, abs/2409.18869, 2024.

Wu, C., Chen, X., Wu, Z., Ma, Y., Liu, X., Pan, Z., Liu, W., Xie, Z., Yu, X., Ruan, C., and Luo, P. Janus: Decoupling visual encoding for unified multimodal understanding and generation. In *CVPR*, pp. 12966–12977. IEEE, 2025a.

Wu, S., Wu, Z., Gong, Z., Tao, Q., Jin, S., Li, Q., Li, W., and Loy, C. C. Openuni: A simple baseline for unified multimodal understanding and generation. *CoRR*, abs/2505.23661, 2025b.

Wu, S., Zhang, W., Xu, L., Jin, S., Wu, Z., Tao, Q., Liu, W., Li, W., and Loy, C. C. Harmonizing visual representations for unified multimodal understanding and generation. In *ICCV*. IEEE, 2025c.

Wu, Y., Zhang, Z., Chen, J., Tang, H., Li, D., Fang, Y., Zhu, L., Xie, E., Yin, H., Yi, L., Han, S., and Lu, Y. VILA-U: a unified foundation model integrating visual understanding and generation. In *ICLR*. OpenReview.net, 2025d.

Xie, J., Mao, W., Bai, Z., Zhang, D. J., Wang, W., Lin, K. Q., Gu, Y., Chen, Z., Yang, Z., and Shou, M. Z. Show-o: One single transformer to unify multimodal understanding and generation. In *ICLR*. OpenReview.net, 2025a.

Xie, J., Yang, Z., and Shou, M. Z. Show-o2: Improved native unified multimodal models. In *NeurIPS*, 2025b.

Xie, R., Du, C., Song, P., and Liu, C. MUSE-VL: modeling unified VLM through semantic discrete encoding. *CoRR*, abs/2411.17762, 2024.

Yang, A., Yang, B., Zhang, B., Hui, B., Zheng, B., Yu, B., Li, C., Liu, D., Huang, F., Wei, H., Lin, H., Yang, J., Tu,

J., Zhang, J., Yang, J., Yang, J., Zhou, J., Lin, J., Dang, K., Lu, K., Bao, K., Yang, K., Yu, L., Li, M., Xue, M., Zhang, P., Zhu, Q., Men, R., Lin, R., Li, T., Xia, T., Ren, X., Ren, X., Fan, Y., Su, Y., Zhang, Y., Wan, Y., Liu, Y., Cui, Z., Zhang, Z., and Qiu, Z. Qwen2.5 technical report. *CoRR*, abs/2412.15115, 2024.

Ye, J., Jiang, D., Wang, Z., Zhu, L., Hu, Z., Huang, Z., He, J., Yan, Z., Yu, J., Li, H., He, C., and Li, W. Echo-4o: Harnessing the power of gpt-4o synthetic images for improved image generation. *CoRR*, abs/2508.09987, 2025.

Yin, S., Fu, C., Zhao, S., Li, K., Sun, X., Xu, T., and Chen, E. A survey on multimodal large language models. *National Science Review*, 11(12):nwae403, 2024.

Yu, W., Yang, Z., Li, L., Wang, J., Lin, K., Liu, Z., Wang, X., and Wang, L. Mm-vet: Evaluating large multimodal models for integrated capabilities. In *ICML*. OpenReview.net, 2024.

Yuan, Y., Li, Z., and Zhao, B. A survey of multimodal learning: Methods, applications, and future. *ACM Comput. Surv.*, 57(7):167:1–167:34, 2025.

Yue, X., Ni, Y., Zhang, K., Zheng, T., Liu, R., Zhang, G., Stevens, S., Jiang, D., Ren, W., Sun, Y., et al. Mmmu: A massive multi-discipline multimodal understanding and reasoning benchmark for expert agi. In *CVPR*, pp. 9556–9567, 2024.

Zhang, C., Zhang, C., Zhang, M., and Kweon, I. S. Text-to-image diffusion models in generative AI: A survey. *CoRR*, abs/2303.07909, 2023.

Zhang, J., Huang, Q., Liu, J., Guo, X., and Huang, D. Diffusion-4k: Ultra-high-resolution image synthesis with latent diffusion models. In *CVPR*, pp. 23464–23473. IEEE, 2025.

Zhou, C., Yu, L., Babu, A., Tirumala, K., Yasunaga, M., Shamis, L., Kahn, J., Ma, X., Zettlemoyer, L., and Levy, O. Transfusion: Predict the next token and diffuse images with one multi-modal model. In *ICLR*. OpenReview.net, 2025.

Zhu, D., Chen, J., Shen, X., Li, X., and Elhoseiny, M. Minigpt-4: Enhancing vision-language understanding with advanced large language models. In *ICLR*. OpenReview.net, 2024.

Zhu, J., Wang, W., Chen, Z., Liu, Z., Ye, S., Gu, L., Tian, H., Duan, Y., Su, W., Shao, J., Gao, Z., Cui, E., Wang, X., Cao, Y., Liu, Y., Wei, X., Zhang, H., Wang, H., Xu, W., Li, H., Wang, J., Deng, N., Li, S., He, Y., Jiang, T., Luo, J., Wang, Y., He, C., Shi, B., Zhang, X., Shao, W., He, J., Xiong, Y., Qu, W., Sun, P., Jiao, P., Lv, H., Wu, L., Zhang, K., Deng, H., Ge, J., Chen, K., Wang, L., Dou, M., Lu, L., Zhu, X., Lu, T., Lin, D., Qiao, Y., Dai, J., and Wang, W. Internvl3: Exploring advanced training and test-time recipes for open-source multimodal models. *CoRR*, abs/2504.10479, 2025.